ESTIMATION OF SHALLOW GEOTHERMAL ENERGY POTENTIAL AT URBAN SCALE: NUMERICAL VS. SEMI-ANAYTICAL MODELS

Charles MARAGNA[1], Fabrice COMPERE[1], Jérôme BARRIERE[1], Camille MAUREL[1], Pascal MONNOT[1]

[1] BRGM, 3 av. Claude-Guillemin 45060 Orléans - France

c.maragna@brgm.fr

Keywords: Ground-source heat pumps, Open loop, numerical modelling, urban planning

ABSTRACT

The assessment of the ground source heat pump (GSHP) potential at urban scale requires taking into account hydraulic and thermal interactions between installations, especially for open loop (groundwater) system. The paper focuses on models for the assessment of aquifer geothermal energy potential in dense urban areas. In such areas, thermal and hydraulic interferences between doublets may arise and tools are needed to optimize the location of the wells. A semi-analytical model is developed to do so and compared to a 3D FEFLOW geothermal model. The underlying restrictive assumptions of the semi-analytical model are discussed, such as the homogeneity of the aquifer. A theoretical maximum density of energy that can be delivered by the GSHP is derived based on maximum acceptable temperature changes at the abstraction wells, and the influence of key parameters (hydraulic transmissivity, productive thickness, regional flow) is investigated, with typical values for Bordeaux Oligocene aquifer.

1. INTRODUCTION

In France, according to the French Energy Environment and Energy Management Agency, nearly 50% of dwellings use gas or fuel oil as primary heating energy while residential and tertiary sectors account for 45% of national final energy consumption and 20% of total greenhouse gas emissions. The French Parliament has promulgated the energy transition law for a green growth in August 2015. This law targets a 40% reduction of greenhouse gas emissions between 1990 and 2030, and renewable energy covering 32% final energy consumption in 2030. Urban areas develop plans to foster the use of renewable energy, including shallow geothermal energy (SGE).

Three urban areas (the conurbations of Paris, Orléans and Bordeaux) requested support from BRGM to foster the use of shallow geothermal energy and ground source heat pump (GSHP) as part of their strategic energy plan. In order to provide a practical tool, BRGM is currently developping a multi-criteria mapping methodology which combines assessment of geothermal resources, maps of thermal energy needs, technological options (such as open loop, borehole or shallow heat exchangers) and an economic criterion (estimation of the heat production cost).

In urban areas, thermal and hydraulic interferences between open-loop systems may arise. The location of the wells and abstracted flow rates need to be optimized so that hydraulic and thermal interferences remain within acceptable ranges. Though methodologies are available to estimate the energy potential of borehole heat exchangers at the levels of a single installation (Casasso and Sethi, 2016) (García-Gil et al., 2015) (Gemelli et al., 2011) or at district level (Zhang et al., 2015), and for open loop at a the level of a single installation (Interreg Alpine Space Greta, 2018), to our knowledge no simple method exist for open loop where interferences between neighboring installations are taking into account.

This paper shows the current development of a model to assess the geothermal energy potential of aquifers in urban areas. It relies on simplified hydrothermal models, which appear to allow a quick computation of hydraulic and thermal interferences and can therefore be integrated into optimization loops to ensure an optimal use of this limited resource. After a reference case has been defined (section 2), a semi-analytical model for open loop systems is developed and validated against a 3D finite element model in FEFLOW (section 3) for a wide range of key parameters. A criteria for the maximum sustainable density of GSHP delivered energy is given in section 4. Applying this criteria, the influence of the aquifer and demand parameters on this density are investigated.

2. REFERENCE CASE

Bordeaux urban area (783,000 inhabitants over 580 km^2) have been considered in this paper, where two shallow aquifers, Oligocene and Eocene, are available for geothermal use. In this sector GSHP have been running for several years, and data are being collected about their operation. Though both aquifers are heterogeneous, typical values can be derived (see Table 1). Both aquifers are confined. Oligocene data serve as a case study.

Table 1 : Typical values for Eocene aquifer in Bordeaux

Parameter	Eocene	Oligocene
Upper cap rock thickness	100 to 250 m	0 to 150 m
Thickness	100 to 150 m	0 to 70 m
Transmissivity	10-3 to 5×10^{-2} m²/s	10-3 to 5×10^{-2} m²/s
Hydraulic gradient	3‰	3‰
Storage coefficient	10^{-4} to 10^{-5}	10^{-4} to 10^{-5}

Table 2 : Nomenclature and reference values (used by default)

	Parameter	Symbol	Unit	Ref. values
General	Hydraulic head	h	m	
	Temperature	T	°C	
	Power	P	W	
	Energy	E	MJ	
	Normalized temperature	T^*	-	
	Darcy velocity	v_D	m.a^{-1}	
	Thermal velocity	v_{th}	m.s^{-1}	
	Complex potential	Ω	m^2.s^{-1}	
Aquifer	Thickness	b	m	30
	Hydraulic conductivity	K	m.s^{-1}	5×10^{-4}
	Storage coefficient	S	-	5×10^{-5}
	Hydraulic gradient	J	-	3‰
	Regional Darcy velocity	$v_{D,\infty}$	m.a^{-1}	47
	Effective porosity	ω	-	0.2
	Aquifer heat capacity	C_a	MJ.K^{-1}.m^{-3}	2.8
	Water heat capacity	C_w	MJ.K^{-1}.m^{-3}	4.12
	Retardation factor	R	-	1
	Media thermal conductivity	λ_m	W.K^{-1}.m^{-1}	2.0
	Longitudinal dispersivity	α_L	m	2
	Transversal dispersivity	α_T	m	0.2
Cap rock	Upper cap rock thickness	d	m	100
	Thermal capacity	C_r	MJ.K^{-1}.m^{-3}	2.2
	Thermal conductivity	λ_r	W.K^{-1}.m^{-1}	2
Wells and operation	Well radius	r_w	m	0.25
	Yearly average flow-rate	$Q_{avg,k}$	m^3.s^{-1}	0.0139
	Heat pump (HP) coefficient of performance	COP	-	4
	Initial temperature	T_0	°C	15
	HP evaporator temperature range	ΔT_{HP}	°C	4
Data specific to benchmark	Distance between extraction and injection well	L	m	80
	Angle between doublet line / regional flow	θ	°	0
	Yearly average flow-rate	Q_{avg}	m^3.s^{-1}	50

3. MODELLING APPROACHES AND BENCHMARK

3.1. Semi-analytical model

3.1.1. Hydrothermal modelling

The semi-analytical model is based on the well-known theory of complex potential. This theory allows computing the streamlines in steady state, and *in fine* the thermal interactions between wells (Javandel and Tsang, 1986) (Luo and Kitanidis, 2004) (Wu et al., 2016) (Milnes and Perrochet, 2013) (Casasso and Sethi, 2015). Though the Oligocene and Eocene are heterogeneous, the model assumes that the aquifer is horizontal, homogeneous and isotropic with a constant thickness, and a regional steady-state flow. The complex potential of a set of doublets with a regional flow reads (Javandel and Tsang, 1986):

$$\underline{\Omega} = \sum_{k=1}^{N} \frac{Q_{avg,k}}{2\pi b} \log\left(\frac{z - z_{E,k}}{z - z_{I,k}}\right) + v_{D,\infty} z = \underline{\Phi} + \mathrm{i}\underline{\psi} \qquad [1]$$

Where $Q_{avg,k} = \int_0^{1\,year} Q_i(t)dt$ is the yearly average flow of doublet k and z is a complex variable defined as $z = x + iy$, with i^2=-1. $z_{E,k}$ and $z_{I,k}$ are the locations of extraction and injection wells of GSHP k respectively. The complex Darcy velocity is given by:

$$\underline{\mathrm{v}_D} = \frac{\partial \underline{\Phi}}{\partial \mathrm{z}} = \sum_{k=1}^{N} \frac{Q_{avg,k}}{2\pi b}\left(\frac{1}{|z - z_{E,k}|} - \frac{1}{|z - z_{I,k}|}\right) + v_{D,\infty} \qquad [2]$$

The streamlines are computed numerically by tracking particles from injection to extraction wells. Eq. [2] can be written as:

$$\frac{\mathrm{d}x}{\mathrm{d}t} = \sum_{k=1}^{N} \frac{Q_{avg,k}}{2\pi b}\left(\frac{x - x_{E,k}}{(x - x_{E,k})^2 + (y - x_{E,k})^2} - \frac{x - x_{I,k}}{(x - x_{I,k})^2 + (y - x_{I,k})^2}\right) + v_{D,\infty}$$

$$\frac{\mathrm{d}y}{\mathrm{d}t} = \sum_{k=1}^{N} \frac{Q_{avg,k}}{2\pi b}\left(\frac{y - y_{E,k}}{(x - x_{E,k})^2 + (y - x_{E,k})^2} - \frac{y - y_{I,k}}{(x - x_{I,k})^2 + (y - x_{I,k})^2}\right) \qquad [3]$$

One defines the thermal feedback (TF) $T^*_{k\to k'}$ by:

$$T^*_{k\to k'}(t) = \frac{T_{k\to k'}(t) - T_0}{T_{in} - T_0} \qquad [4]$$

The TF is determined numerically: The initial temperature is set to 0 in the whole domain, while the injection temperature is 1 for every injection well. N particles (e.g. N = 100) are released at t = 0 in every injection well. These particles are evenly distributed around the injection well perimeter. The trajectory of every particle is computed by solving eq. [3] with a Runge-Kutta (RK4-5) numerical scheme. The flow between two streamline connecting injection well I_k to extraction well $E_{k'}$, the flowrate remains constant and equal to $Q_{avg,k}/N$.

Assuming an infinite extent of the cap rock, for every streamline ψ_i connecting I_k and $E_{k'}$, the evolution of the thermal feedback is (Gringarten and Sauty, 1975):

$$\left(T_{\psi_i}{}^*\right)_{k\to k'}(t) = \mathrm{H}(t - t_{tb,\psi})\mathrm{erfc}\left(\left(\frac{{C_w}^2}{\lambda_r C_r}\left(\frac{Q_{avg,k}/N}{A_\psi}\right)^2 (t - t_{tb,\psi})\right)^{-\frac{1}{2}}\right) \qquad [5]$$

where H the Heaviside function and $t_{tb,\psi}$ is the thermal breakthrough time relative to the streamline ψ_i,

corresponding to the thermal front of the streamline reaching the extraction well:

$$t_{tb,\psi} = \frac{C_a}{C_w}\frac{bA_\psi}{(Q_{avg,k}/N)} \quad [6]$$

A_ψ is for the horizontal surface of a channel bounded between two adjacent streamlines ψ_i *and* ψ_{i+1}. $bA_\psi/(Q_{avg,k}/N)$ is indeed the time to "fill" this channel. The thermal feedback from I_k to $E_{k'}$ is obtained by summing the contributions from every streamline ψ_i connecting these two wells:

$$T^*_{k\to k'}(t) = \frac{1}{N}\sum_i \left(T_{\psi_i}{}^*\right)_{k\to k'}(t) \quad [7]$$

3.1.2. Integration with the surface installation (heat pump)

One considers that the GSHP delivers only heating, and no cooling requirement is taken into account at this point. The calorific power P_{cal} and the frigorific energy P_{fr} retrieved from the ground at any time *t* are:

$$P_{fr}(t) = Q_k(t)\Delta T_{HP} C_w$$
$$P_{cal}(t) = \frac{P_{fr}}{\left(1-\frac{1}{COP}\right)} \quad [8]$$

Where ΔT_{HP} is the temperature difference at the HP evaporator. Yearly calorific and frigorific energies $E_{cal,HP}$ and $E_{fr,HP}$ are :

$$E_{fr} = Q_{avg,k}\Delta T_{HP} C_w \Delta t_y$$
$$E_{cal} = \frac{E_{fr}}{\left(1-\frac{1}{COP}\right)} \quad [9]$$

with Δt_y = 1 year. The coefficient of performance of the heat pump is assumed to be constant. Note that this is an approximation, since COP will change with the extraction temperature.

The time is discretized in time steps Δt (here Δt = 1 week). For every time step, the heat demand $P_{cal,HP}(t)$ is aggregated into $P_{cal,HP}{}^n$. The streamlines and thermal feedback have been computed assuming a constant flowrate. Since in real conditions the flowrate will vary, an "equivalent" difference temperature $(\Delta T_{HP})_{eq,k}{}^n$ is computed so that the energy is conserved during time step *n*:

$$(\Delta T_{HP})_{eq,k}{}^n = T_{in,k}{}^n - T_{out,k}{}^n \approx \frac{P_{fr}{}^n}{E_{fr}}\Delta T_{HP}\Delta t_y \quad [10]$$

As the breakthrough time is much larger than the time step, *e.g.* several months against 1 week, eq. [10] can be approximated by:

$$T_{in,k}{}^n \approx T_{out,k}{}^{n-1} - (\Delta T_{HP})_{eq,k}{}^n \quad [11]$$

Eq. [11] means that the extraction temperature a time step *n* is not affected by the injection temperature in the same time step. At every time step *n*, the extraction temperatures are computed as follows: one first computes the injection temperatures (eq. [11]). As the underlying heat equation is linear, multiple interacting installations can be accounted for by the space superimposition principles. The extraction temperatures $T_{out,k}{}^n$ are computed by summing the contribution from every injector. Time-varying injection temperatures are dealt with by the time superposition principle, which leads to:

$$T_{out,k}{}^2 = T_0 + \sum_{k'} T_{in,k'}{}^1 T^*_{k'\to k}{}^1 \text{ if } n = 2$$
$$T_{out,k}{}^n = T_0 + \sum_{k'} T_{in,k'}{}^1 T^*_{k'\to k}{}^n + \sum_{k'}\sum_{m=2}^{n}\left(T_{in,k'}{}^m - T_{in,k'}{}^{m-1}\right) T^*_{k'\to k}{}^{n+1-m} \text{ if } n > 2 \quad [12]$$

The sum over *k'* is related to the every injection well *k'* connected to the extraction well *k*. One may have *k'* = *k*, which means that injection and extraction wells are within the same GSHP. The simulation time is 25 years. The above mentioned equations have been solved numerically by a programme implemented in Matlab®. The execution time is about 1 second per GSHP.

3.1.3. Hydraulic interferences between the wells

The well screen is supposed to go through the whole aquifer. When the flow rate Q is constant, the change of hydraulic head Δh at a radial distance *r* from a well can be estimated with Theis equation:

$$\frac{\Delta h}{Q} = \frac{1}{4\pi Kb}\mathrm{E}_1\left(\frac{Sr^2}{4Kbt}\right) = G(r,t) \quad [13]$$

with:

$$\mathrm{E}_1(u) = \int_u^\infty \frac{e^{-u}}{u}du \quad [14]$$

The evolution of the hydraulic head in the vicinity of any well *k* can be computed with the time and space superimposition principles, as for eq. [12].

3.2. Benchmark: semi-analytical approach vs. FeFlow model

The semi-analytical model was compared to an open-loop geothermal system developed in the finite-element code FEFLOW® 7.2 (DHI-WASY, Berlin, Germany). The metrics for the comparison is the evolution of the thermal feedback.

The benchmark case is a single doublet aligned in the direction of the regional water flow, the extraction well being upstream (see Table 2). When both conditions are met (Lippmann and Tsang, 1980) introduces a *X* parameter defined by:

$$X = \frac{2Q_{avg}}{\pi bkJL} \quad [15]$$

If X is larger than 1, no thermal feedback will occur. With the numerical values given in Table 2, X = 2.45, which will cause a certain amount of thermal feedback between the extraction and injection wells.

3.2.1. FeFlow model

The default horizontal dimensions of the FeFlow model were 2000 m x 2000 m, centred around the abstraction well (coordinates x,y = 0,0) and the reinjection well (coordinates x,y = 80,0).

Assuming a fully confined system, the model was composed of three main geological formations: the aquifer with a thickness of b = 30 m (vertically discretized with layers 1.25 m thick), and an upper (cap rock) and down formations, each one with a default thickness d = 100 m (vertically discretized with layers 10 m thick). For simulations involving a reduction of the upper cap rock thickness, the thickness of each constitutive layer of this formation was reduced to 2 m.

A triangular mesh was generated with the "Triangle method" available in FeFlow, with an higher meshing density around the wells (inner domain of 1000 m x 1000 m) ensuring a better numerical stability. The resulting mesh consisted of layers containing each one 156,224 elements and 78,369 nodes.

First-kind/Dirichlet boundary condition (imposed hydraulic head) were applied on the western (upgradient) and eastern (downgradient) borders of the model, to reproduce the groundwater flow.

To compute the initial hydraulic head distribution (without well operation) the model was run in steady state, with an homogeneous hydraulic conductivity K = 5.10^{-4} m.s^{-1} for the aquifer, and 10^{-8} m.s^{-1} for the upper and underlying formations.

The extraction and injection wells were introduced in the model as Multilayer Wells (fourth-kind boundary condition), screened throughout the entire aquifer.

The model was extended to a transient flow and transient heat-transport model running for a simulation time of 25 years, with a constant pumping/reinjection rate of 1,200 m3/day. The initial temperature over the whole domain was set with a groundwater temperature of 0°C. As the groundwater entering the model domain is assumed to have the same temperature of 0°C, first-kind/Dirichlet boundary condition was imposed on the western border ; the same boundary condition was applied on the upper slice of the model.

To simulate the effect of the single doublet, a constant temperature of 1°C (first-kind/Dirichlet boundary condition) was applied over all the nodes of the reinjection well.

3.2.2. Analytical considerations

Note that if the cap rock is perfectly insulated (λ_r = 0), the normalized temperature (eq. [5]) reduces to:

$$T_\psi{}^*(t) = \mathrm{H}\left(t - t_{tb,\psi}\right) \qquad [16]$$

In this specific case, the thermal breakthrough time t_{tb} and thermal feedback $T_{12}^{*\,\infty}$ in steady state have been analytically derived (Milnes and Perrochet, 2013):

$$t_{tb} = \frac{C_a}{C_w}\frac{L}{KJ}\left(\frac{X}{\sqrt{X-1}}\operatorname{atan}\left(\frac{1}{\sqrt{X-1}}\right) - 1\right)$$
$$T_{1\to 2}^{*\,\infty} = \frac{2}{\pi}\left(\operatorname{atan}\left(\sqrt{X-1}\right) - \frac{\sqrt{X-1}}{X}\right) \qquad [17]$$

Setting λ_r = 0, the semi-analytical model has been checked against these values for the reference case. Eq. [17] and the numerical model yield t_{tb} = 171 days (resp. 168 days) and $T_{12}^{*\,\infty}$ = 0.247 (resp. 0.242).

3.2.3. Results and discussion

Both semi-analytical and FeFlow models appear to be in good to excellent agreement, the discrepancy of the long-term thermal feedback being 1 % at most. The most significant difference between approaches appears at the beginning of the thermal breakthrough. The SA model then leads to sharper temperature changes due to the fact it does not account for thermal dispersivity, as does the FeFlow model (see Figure 1). Both models are in good agreement for a wide range of aquifer thickness and Darcy velocities (see Figure 1 and Figure 2).

The aquifer top depth d is not taken into account by the semi-analytical approach which considers a cap rock of infinite extent. When the aquifer is shallow (e.g. d = 10 m) the thermal feedback computed by the FE model is c.a. 3% lower than for the reference case, since heat is transferred through the ground surface (see Figure 3). However, this thermal recharge remains limited. This does not appear to be in line with previously published works, which suggest that shallow aquifers are largely affected by the ground temperature (Piga et al., 2017). One explanation may be that Piga et al. studied the plume downwards on a much longer distance (several hundreds of meters) than the well distance in our case study (L = 80 m). In any case, the influence of the aquifer depth must be further investigated, and appropriate semi-analytical models derived.

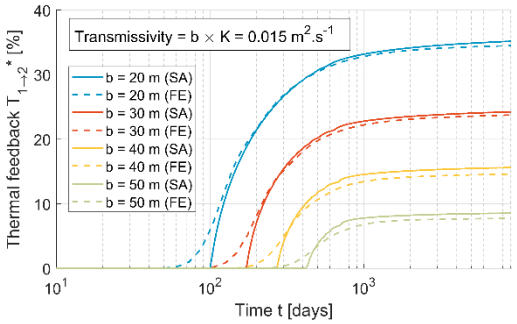

Figure 1 : Comparison of the thermal feedback computed by the semi-analytical (SA) and finite elements (FE) methods for several values of aquifer thickness *b*, the transmissivity being constant. Reference case is *b* = 30 m.

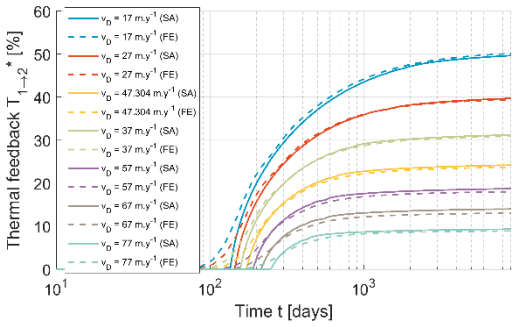

Figure 2 : Comparison of the thermal feedback: Influence of Darcy velocity v_D. The hydraulic conductivity *K* remains unchanged (5×10^{-4} m.s^{-1}), while the hydraulic gradient is adjusted. Reference case is v_D = 47 m.y^{-1}.

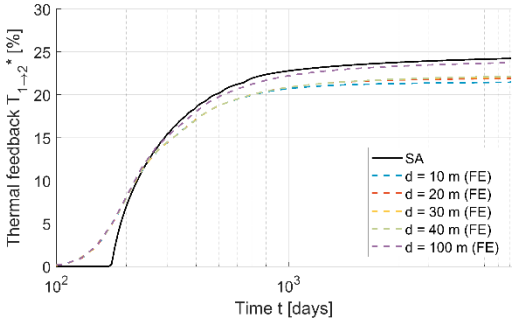

Figure 3 : Comparison of the thermal feedback: Influence of the aquifer top depth *d*. Reference case is *d* = 100 m.

4. MAXIMUM DENSITY OF ENERGY DELIVERD BY THE GSHP

Thermal interferences and long-term temperatures drift arising between GHSP, or even between the injection and extraction wells of the same installation, may jeopardize the efficiency of the heat pump. Hydraulic interferences may cause flooding if not properly assessed.

We defined a synthetic case to estimate how neighbouring GSHP will be thermally and hydraulically affected by each other. We performed a parametric study to estimate how the extraction temperatures and hydraulic heads in the wells are affected by the heat demand density, the aquifer parameters, etc.

4.1. Definition of a synthetic case

We defined with a neighbourhood with N square plots of width D_p = 150 m, with a square building of width D_b = 75 m right in the middle (see Figure 4). Each building has its own GSHP, with one production and one injection well, located at 5 m from the building well, upstream for the extraction well, downstream for the injection well. The distance between the injection and extraction well of a single installation is therefore 85 m. There are N_x plots in the direction of the underground water flow (Ox) and N_y plots in the transversal direction (Oy) so that $N = N_x \times N_y$. To minimize thermal interferences wells, the production and injection wells of every GSHP are parallel to the (Ox) axis, with the injection well being downstream. The wells are shifted in the (Oy) direction from one installation to the other when going to the right (downstream), so that to avoid the GSHP downstream is in the thermal plume of the GSHP upstream. The building demand has been estimated by POLITO within the Interreg Alpine Space GRETA project. This a poorly insulated accommodation located in Torino. Given the climate classification defined within GRETA project, Torino climate is the closest to Bordeaux climate in terms of heating degree-days. The heating demand of such a house is 4.05 MWh.y^{-1}. In our simulations, the heating demand of the single house is scaled to meet any given heating demand we want to investigate (see Figure 5).

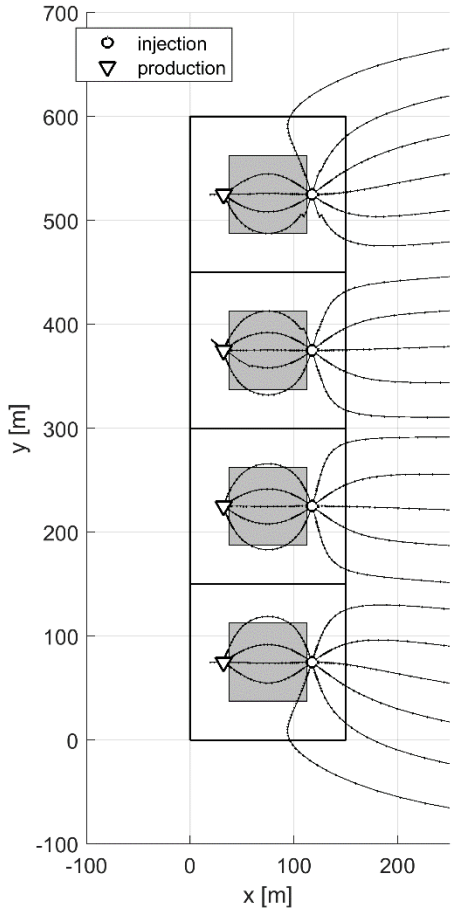

Figure 4 : Map of the synthetic case showing selected streamlines. N_x = 1, N_y = 4. $E_{cal,HP}$ = 3500 MWh.y^{-1}.

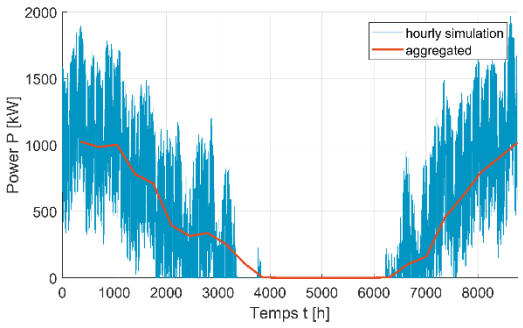

Figure 5 : Heat demand: Original hourly heat demands and aggregated profiles used for the simulations (weekly averaged values). $E_{cal,HP}$ = 3500 MWh.y^{-1}.

The influence of the calorific energy delivered by each GSHP $E_{cal,HP}$ has been investigated from 500 MWh.y^{-1} to 3500 MWh.y^{-1}, along with the number of plots and their disposal in the *x* and *y* direction (N_x = 1, N_y =1 ; N_x = 4, N_y =1; N_x = 1, N_y =4 ; N_x = 3, N_y = 3 ; N_x = 4, N_y =4).

For every simulation, the thermal interferences have been estimated by plotting the energy produced by every GSHP as a function of the temperature change regarded to the initial temperature. For instance, for 4 GSHP oriented in the direction of the water flow, the temperature change remains below 3.5 °C when every installation delivers 1 000 MWh.y^{-1}. However, increasing the demand by 50 % causes the most downstream installation to be experience temperature changes up to 6 K (see Figure 6).

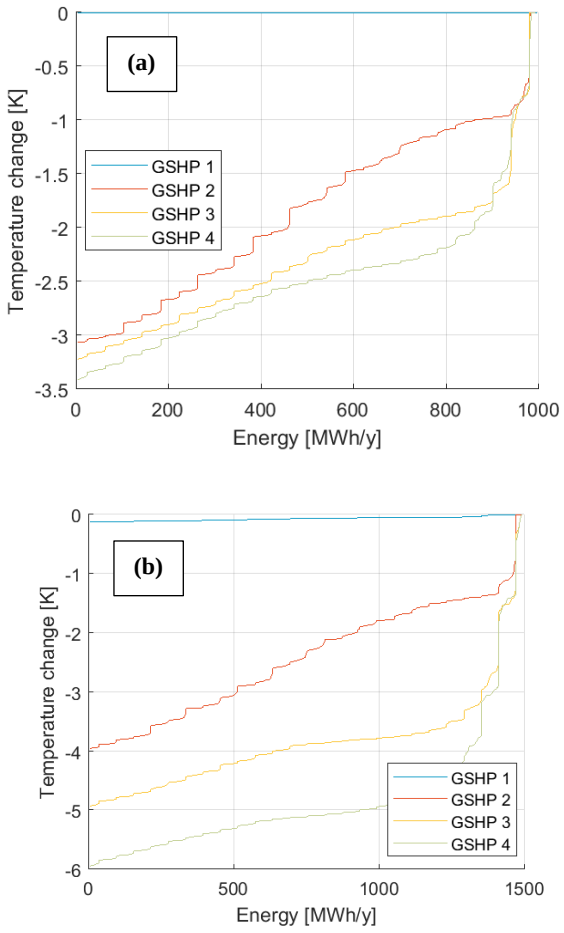

Figure 6 : Temperature of the heat produced by each GSHP. N_x = 4, N_y = 1, for $E_{cal,HP}$ = 1000 MWh.y^{-1} (a) and $E_{cal,HP}$ = 1500 MWh.y^{-1} (b). GHSP are labelled downstream (GSHP 1 is upstream, GSHP 4 downstream).

The mean and maximum temperature changes of the distribution of the energy produced by every GSHP have been derived. These two key indicators are deeply affected by the delivered heat and the plots configuration (see Figure 7). .

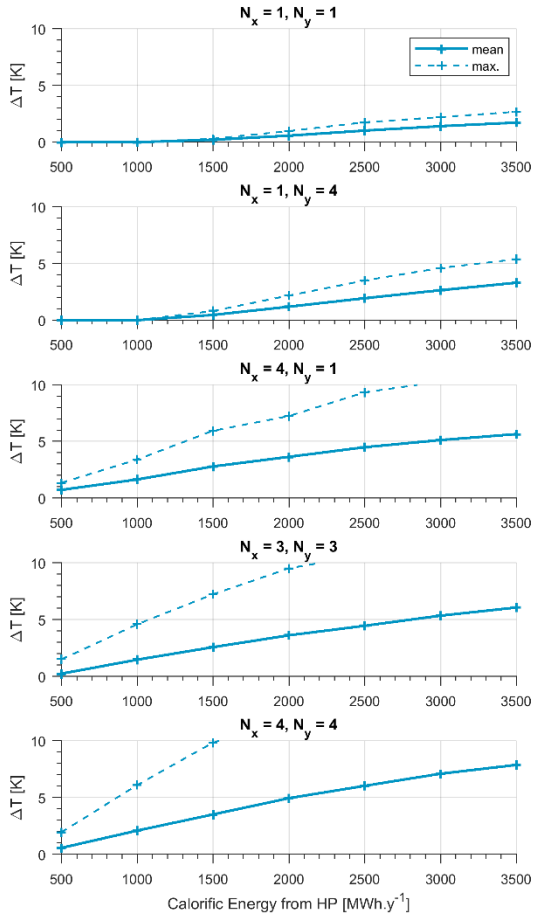

Figure 7 : Mean and maximum temperature changes as a function of the calorific energy delivered by the heat pump, for several combinations of N_x and N_y parameters. For the sake of clarity, the vertical axis is set to 0-10 K range.

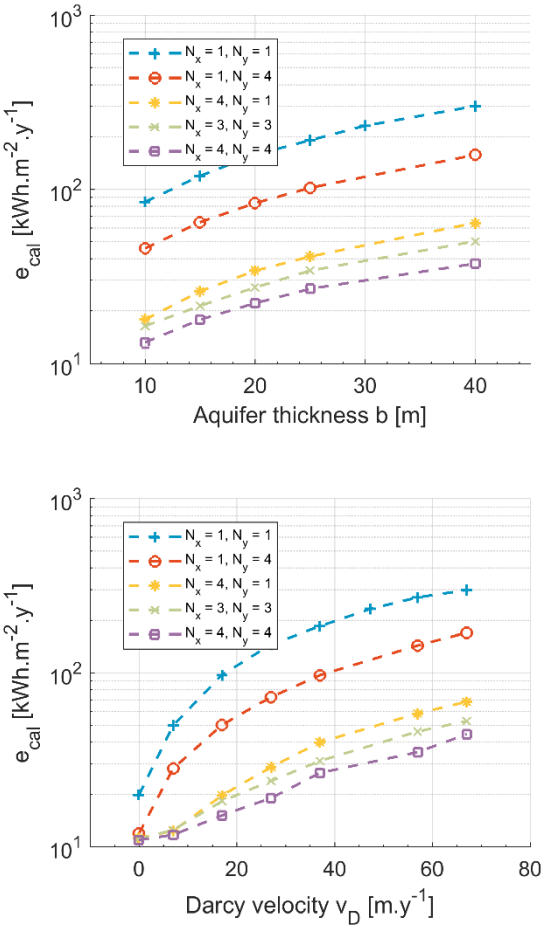

Figure 8 : Energy density as a function of aquifer thickness and Darcy velocity for several plot configurations.

To estimate the maximum density of operations, the following criteria has been set: the maximum temperature change shall not exceed 4 K. This threshold has been chosen by analogy with the French regulation regarding shallow geothermal energy. This regulation offers a simplified declarative regime if among other factors the temperature change at 200 m from the wells does not exceed 4 K. Accepting a larger temperature change would result in a larger density energy that can be covered by GSHP. This maximum density of energy is defined by the amount of energy the HP can cover $E_{cal,HP}$ divided by the surface of a plot (150 m × 150 m = 2.25 ha). Indeed, this energy density varies by more than 2 orders of magnitude related (see Figure 8). Configurations with a single isolated GSHP can deliver a much larger amount of energy, since most of the cold water is evacuated down the installation. For the densest configurations (N_x = 3, N_y = 3 and N_x = 4, N_y = 4), increasing the Darcy velocity from 0 to c.a. 70 m.y^{-1} allows multiplying the energy density by c.a. 3 to 4, or similarly if the aquifer thickness increases from 10 m to 40 m.

CONCLUSION

The developed semi-analytical model allows to assess the thermal and hydraulic interactions. Its application to a reference case shows that the amount of energy one can extract from shallow aquifers is heavily dependent on parameters such as the GSHP density, the aquifer thickness and the Darcy velocity. This model needs to be further developed before it is applied to agglomeration scale. By order of priority, next step will be the following:

i) **Model verification:** The model has been benchmarked against FeFlow for constant injection temperatures and flow-rates. It now needs to be validated for time-varying flow-rates.

ii) **Model representativeness and boundary conditions:** The semi-analytical model assumes a semi-infinite cap rock, though shallow aquifers are affected by the surface thermal regime, as has been observed in Basel (Mueller et al., 2018), Cologne and Winnipeg (Zhu et al., 2011). More representative models will be derived.

iii) **Cooling:** Only the heating demand has been regarded so far. Balanced cooling and heating demands can indeed avoid long-term drift of the ground temperature. We will evaluate how the number of GSHP installations can be densified by balanced heating and cooling demands.

iv) **Heterogeneity:** aquifer heterogeneity (including transmissivity) will have to be taken into account.

v) **Optimization:** The locations of the wells have been defined by a rule of the thumb to minimize thermal recycling, while all GSHP extracted the same amount of heat. In the future the model will be coupled with optimisation algorithms so that to maximize the amount of heat extracted in a given area by adjusting the wells locations and flow-rates.

Besides the integration of the semi-analytical model into a **Geographical Information System** (GIS) like for instance QGIS would be useful for public and local administration to evaluate interferences and deliver permits and authorizations.

REFERENCES

Casasso, A., Sethi, R., 2016. G.POT: A quantitative method for the assessment and mapping of the shallow geothermal potential. Energy 106, 765–773. https://doi.org/10.1016/j.energy.2016.03.091

Casasso, A., Sethi, R., 2015. Modelling thermal recycling occurring in groundwater heat pumps (GWHPs). Renew. Energy 77, 86–93. https://doi.org/10.1016/j.renene.2014.12.003

García-Gil, A., Vázquez-Suñe, E., Alcaraz, M.M., Juan, A.S., Sánchez-Navarro, J.Á., Montlleó, M., Rodríguez, G., Lao, J., 2015. GIS-supported mapping of low-temperature geothermal potential taking groundwater flow into account. Renew. Energy 77, 268–278. https://doi.org/10.1016/j.renene.2014.11.096

Gemelli, A., Mancini Adriano, A., Longhi, S., 2011. GIS-based energy-economic model of low temperature geothermal resources: A case study in the Italian Marche region. Renew. Energy 36, 2474–2483. https://doi.org/10.1016/j.renene.2011.02.014

Gringarten, A.C., Sauty, J.P., 1975. A theoretical study of heat extraction from aquifers with uniform regional flow. J. Geophys. Res. 80, 4956–4962. https://doi.org/10.1029/JB080i035p04956

Interreg Alpine Space Greta, 2018. Local-scale maps of the NSGE potential in the Case Study areas.

Javandel, I., Tsang, C. -F, 1986. Capture-Zone Type Curves: A Tool for Aquifer Cleanup. Groundwater 24, 616–625. https://doi.org/10.1111/j.1745-6584.1986.tb03710.x

Lippmann, M.J., Tsang, F.C., 1980. Ground-Water Use for Cooling: Associated Aquifer Temperature Changes. Ground Water 18. https://doi.org/https://doi.org/10.1111/j.1745-6584.1980.tb03420.x

Luo, J., Kitanidis, P.K., 2004. Fluid residence times within a recirculation zone created by an extraction-injection well pair. J. Hydrol. 295, 149–162. https://doi.org/10.1016/j.jhydrol.2004.03.006

Milnes, E., Perrochet, P., 2013. Assessing the impact of thermal feedback and recycling in open-loop groundwater heat pump (GWHP) systems: a complementary design tool. Hydrogeol. J. 21, 505–514. https://doi.org/10.1007/s10040-012-0902-y

Mueller, M.H., Huggenberger, P., Epting, J., 2018. Combining monitoring and modelling tools as a basis for city-scale concepts for a sustainable thermal management of urban groundwater resources. Sci. Total Environ. 627, 1121–1136. https://doi.org/10.1016/j.scitotenv.2018.01.250

Piga, B., Casasso, A., Pace, F., Godio, A., Sethi, R., 2017. Thermal impact assessment of groundwater heat pumps (GWHPs): Rigorous vs. simplified models. Energies 10. https://doi.org/10.3390/en10091385

Wu, B., Zhang, X., Jeffrey, R.G., Bunger, A.P., Jia, S., 2016. A simplified model for heat extraction by circulating fluid through a closed-loop multiple-fracture enhanced geothermal system. Appl. Energy 183, 1664–1681. https://doi.org/10.1016/j.apenergy.2016.09.113

Zhang, Y., Choudhary, R., Soga, K., 2015. Influence of GSHP system design parameters on the geothermal application capacity and electricity consumption at city-scale for Westminster, London. Energy Build. 106, 3–12. https://doi.org/10.1016/j.enbuild.2015.07.065

Zhu, K., Blum, P., Ferguson, G., Balke, K.-D., Bayer, P., 2011. The geothermal potential of urban heat islands. Environ. Res. Lett. 6, 019501. https://doi.org/10.1088/1748-9326/6/1/019501